

Electronic Supplementary Information (ESI)

The impact of microstructural features of carbon support on the electrocatalytic hydrogen evolution reaction

Munzir. H. Suliman,^{a,b} Alaaldin Adam,^a Mohammad N. Siddiqui,^b Zain H. Yamani,^a Mohammad Qamar,^{*a}

^aCenter of Excellence in Nanotechnology (CENT), ^bDepartment of Chemistry, King Fahd University of Petroleum and Mineral, Dhahran 31261, Saudi Arabia.

*Corresponding author – qamar@kfupm.edu.sa

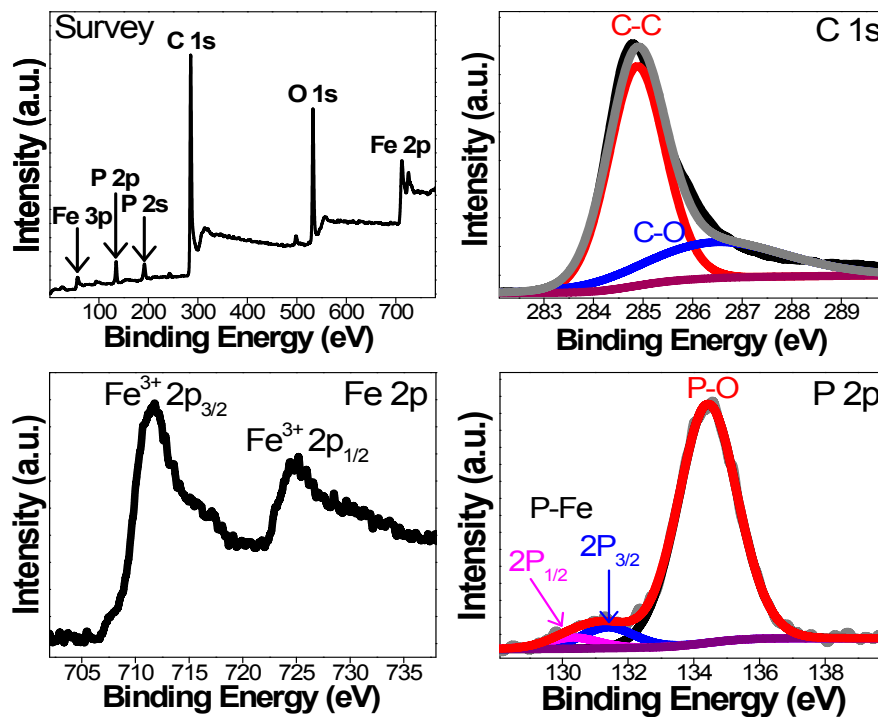


Fig. S1 XPS signatures of FeP/CNT.

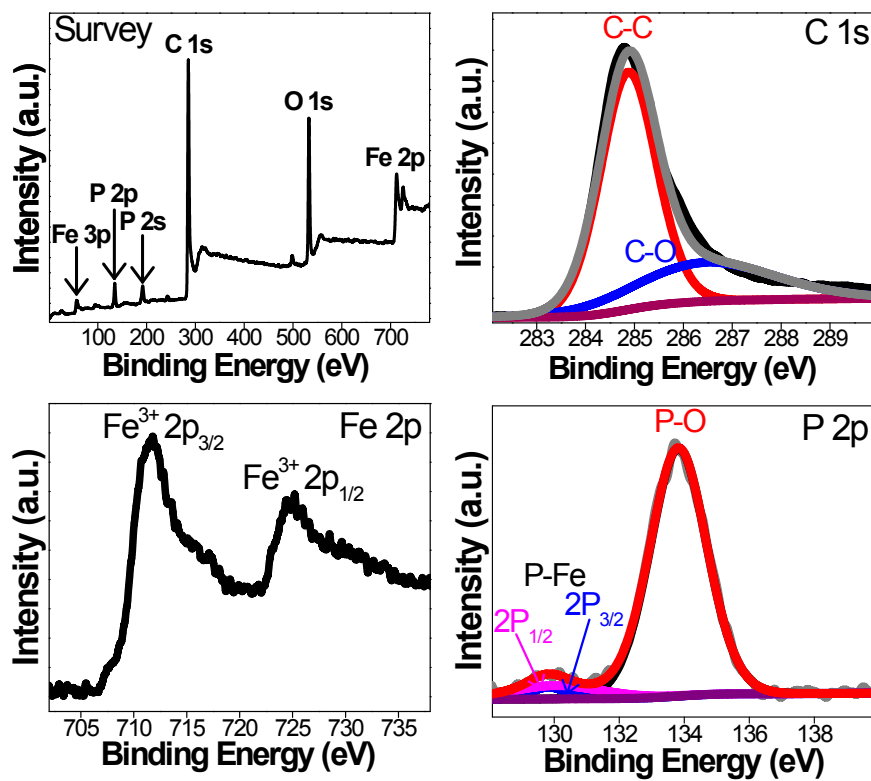


Fig. S2 XPS signatures of FeP/XC.

Table S1 Results of elemental analyses of FeP/CN, FeP/CNT and FeP/XC.

| Electrocatalyst | Theoretical composition | | | Calculated composition | | |
|-----------------|-------------------------|------|------|------------------------|------|------|
| | Fe% | P% | C% | Fe% | P% | C% |
| FeP/CN | 33.1 | 17.4 | 49.5 | 32.4 | 20.3 | 47.3 |
| FeP/CNT | 33.1 | 17.4 | 49.5 | 32.9 | 20.2 | 46.9 |
| FeP/XC | 33.1 | 17.4 | 49.5 | 32.6 | 18.8 | 48.6 |

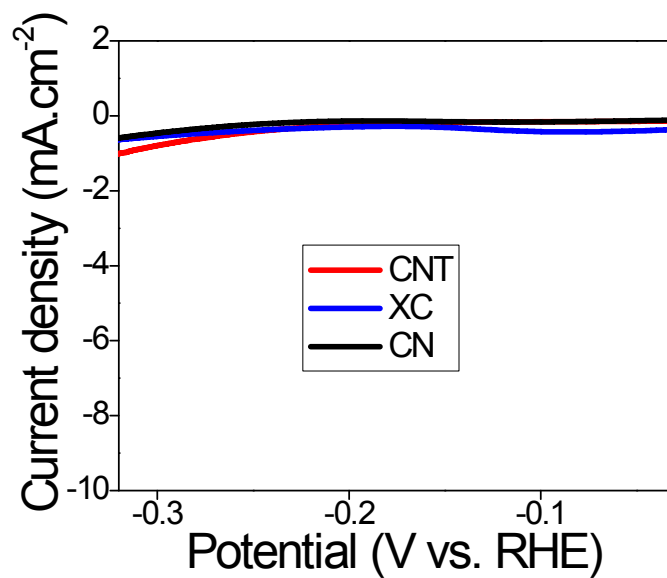


Fig. S3 Comparative polarization curves of pure XC, CNT and CN in 0.5 M H₂SO₄.

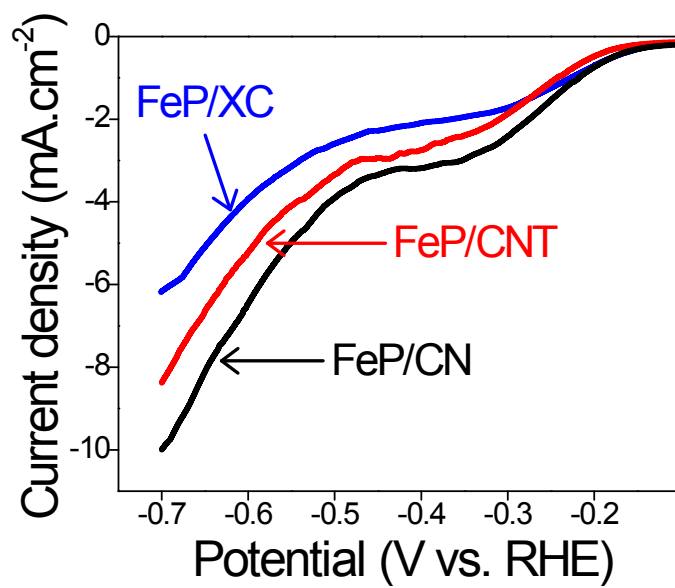


Fig. S4 Comparative polarization curves of FeP/XC, FeP/CNT and FeP/CN in phosphate buffer pH 7.

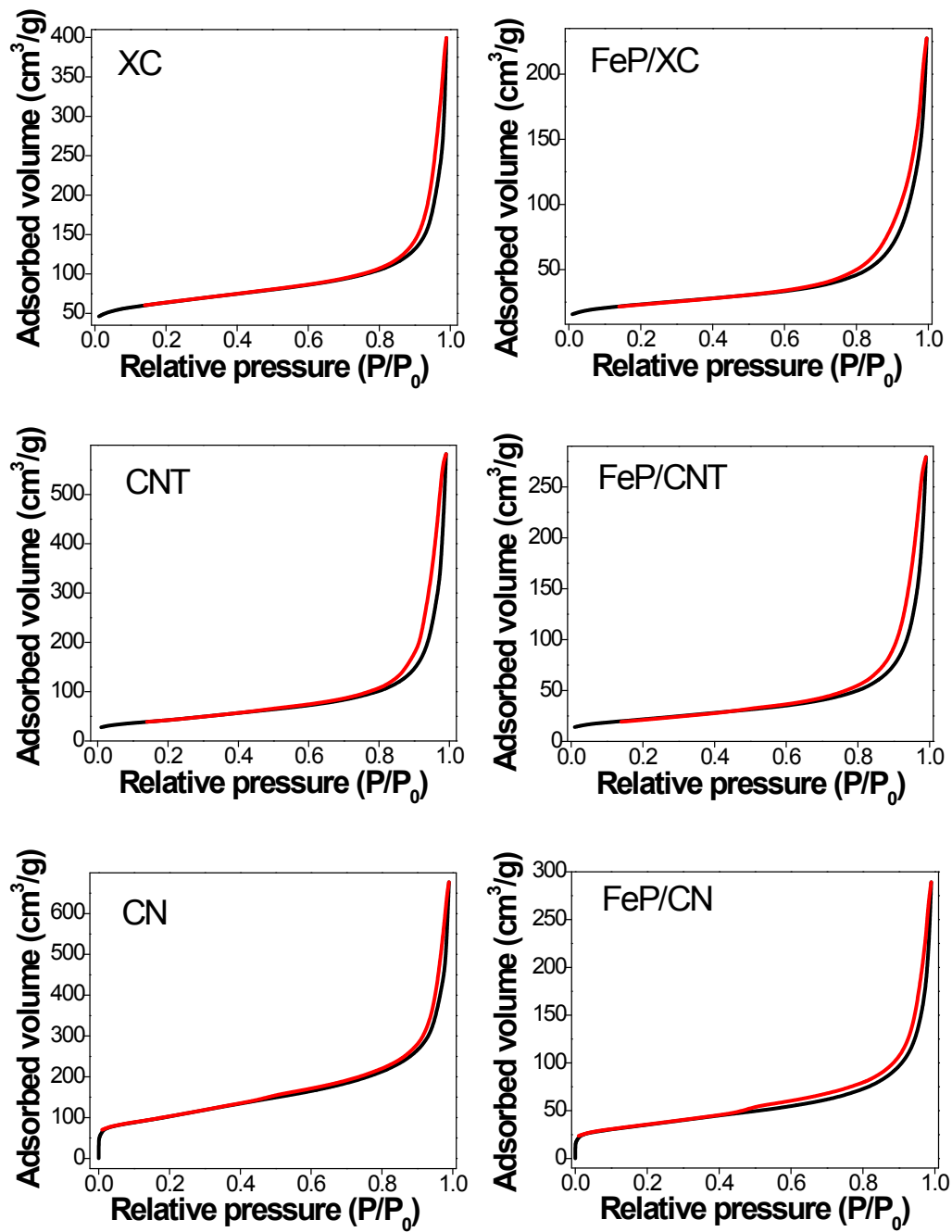


Fig. S5 Nitrogen adsorption-desorption isotherms of pristine carbon and FeP-modified carbon.

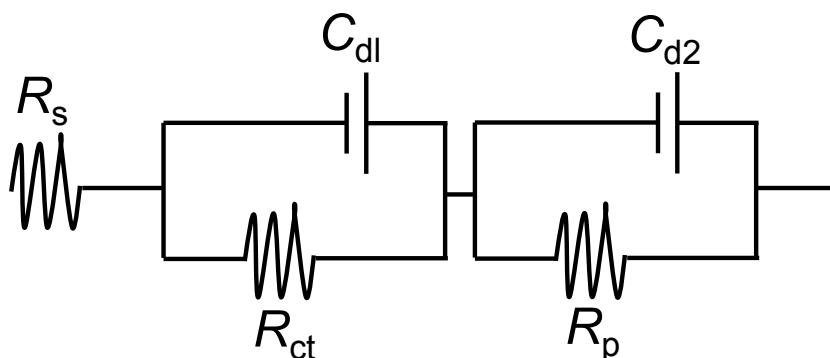


Fig. S6 Two time constant electrical equivalent circuit model utilized to fit the electrochemical impedance (EIS) results of hydrogen evolution reaction. R_s – series resistance, C_{dl} and C_{d2} are double layer capacitance, R_{ct} – charge transfer resistance for HER, R_p – resistance related to the surface porosity.

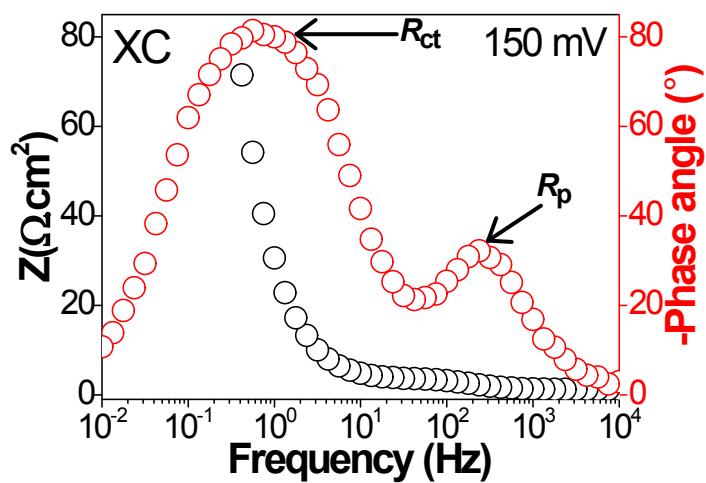


Fig. S7 Representative Bode plot of pristine XC carbon electrodes showing the presence of two-time constants.

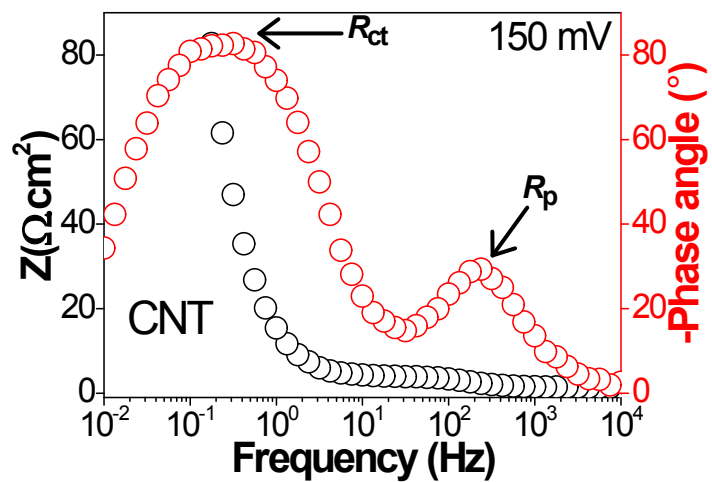


Fig. S8 Representative Bode plot of pristine CNT electrode showing the presence of two-time constants.

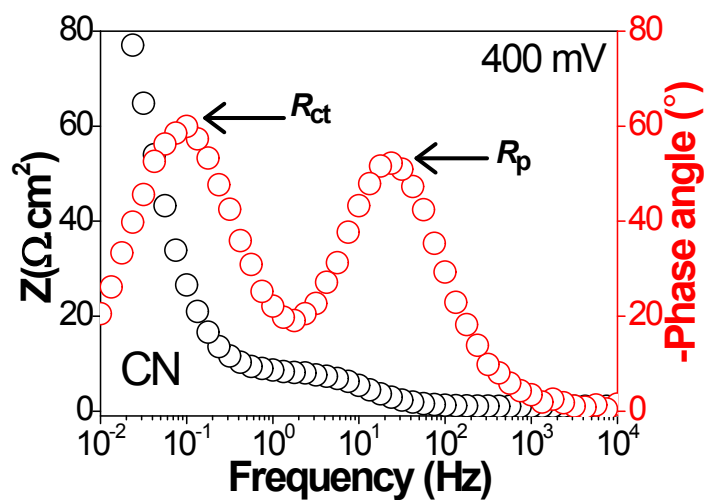


Fig. S9 Representative Bode plots of pristine nanosheets electrode showing the presence of two-time constants.

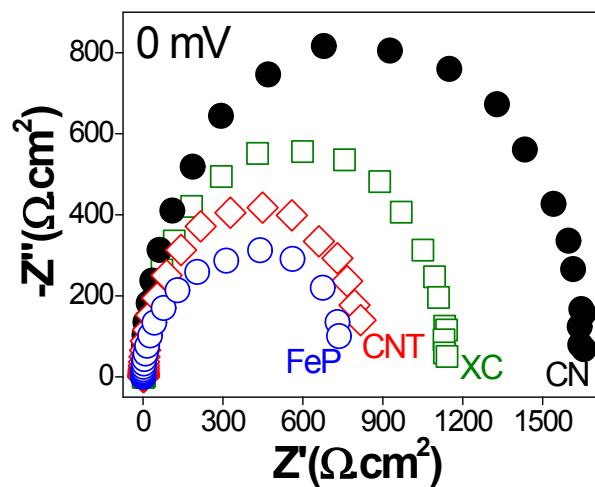


Fig. S10 Nyquist plots of pristine carbon and FeP electrodes showing intrinsic electrical conductivity.

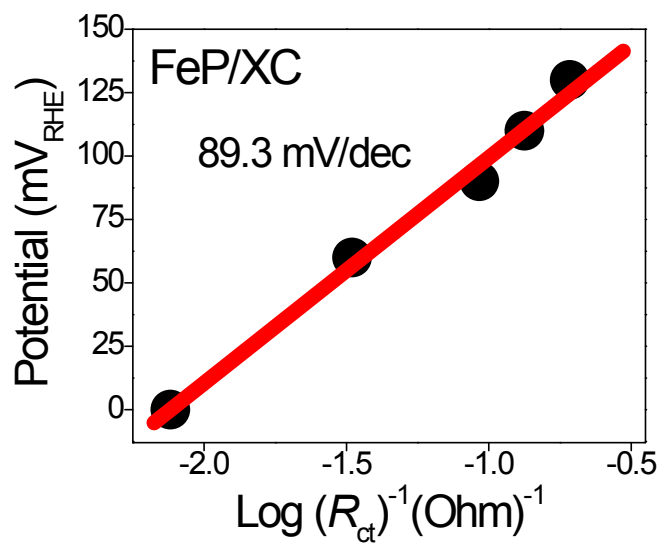


Fig. S11 Tafel slope of FeP/XC.

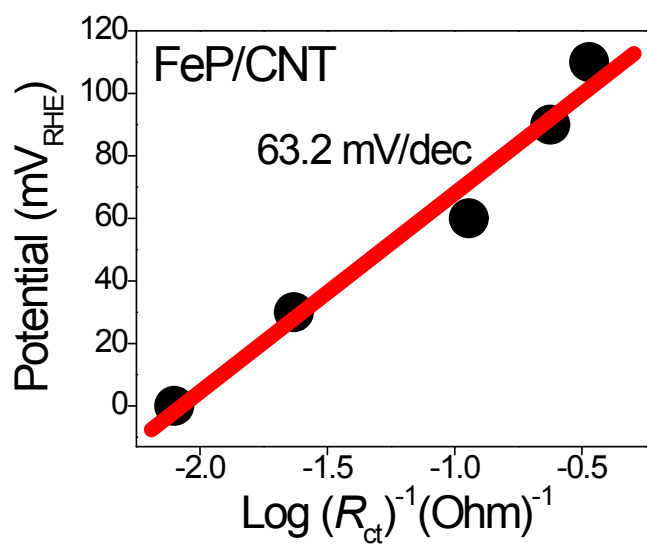


Fig. S12 Tafel slope of FeP/CNT.

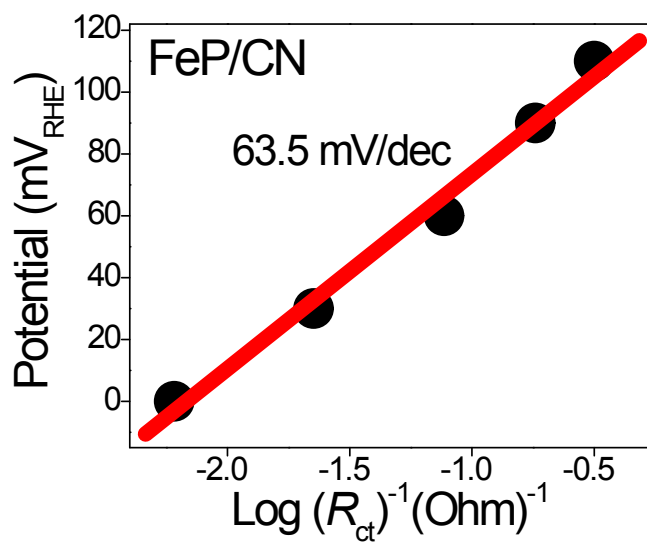


Fig. S13 Tafel slope of FeP/CN.

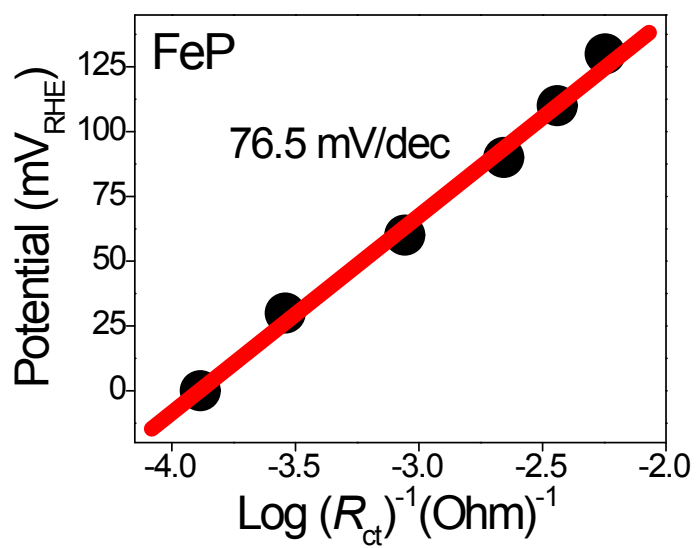


Fig. S14 Tafel slope of pure FeP.

Table S2 Electrochemical impedance values of pristine carbon and pure FeP obtained by fitting their Nyquist Plots.

| Potential (mV) | CN | | | CNT | | | XC | | | FeP | |
|-------------------|-------|------------------------|----------|-------|------------------------|----------|-------|------------------------|----------|-------|---------------------------|
| | R_s | R_p $\Omega.cm^2$ | R_{ct} | R_s | R_p $\Omega.cm^2$ | R_{ct} | R_s | R_p $\Omega.cm^2$ | R_{ct} | R_s | R_{ct} $\Omega.cm^2$ |
| 0 | 3.32 | 5.91 | 1685 | 0.72 | 1.22 | 860.7 | 0.88 | 1.42 | 1146 | 0.87 | 785.3 |
| 30 | 3.29 | 6.30 | 1520 | 1.12 | 1.30 | 804.5 | 0.83 | 1.50 | 870.7 | 0.85 | 457.7 |
| 60 | 3.07 | 5.8 | 1408 | 0.86 | 1.54 | 603.1 | 0.71 | 1.26 | 788.3 | 0.81 | 99.3 |
| 90 | 2.87 | 5.48 | 1323 | 0.57 | 1.00 | 403.9 | 0.78 | 1.03 | 731.8 | 0.83 | 58.5 |
| 110 | 2.35 | 5.3 | 1207 | 1.48 | 1.25 | 357.3 | 1.13 | 1.30 | 657 | 0.88 | 31.8 |
| 130 | 2.76 | 4.67 | 1126 | 0.76 | 1.45 | 243.5 | 1.21 | 1.76 | 612.9 | 0.73 | 16.4 |
| 150 | 2.44 | 5.5 | 1006 | 1.03 | 1.30 | 97.7 | 1.23 | 1.30 | 563.2 | 0.77 | 11.6 |

Table S3 Electrochemical impedance values of FeP-modified carbon obtained by fitting their Nyquist Plots.

| Potential (mV) | FeP/CN | | | FeP/CNT | | | FeP/XC | | |
|-------------------|--------|---|----------|---------|---|----------|--------|---|----------|
| | R_s | R_p ($\Omega \cdot \text{cm}^2$) | R_{ct} | R_s | R_p ($\Omega \cdot \text{cm}^2$) | R_{ct} | R_s | R_p ($\Omega \cdot \text{cm}^2$) | R_{ct} |
| 0 | 0.99 | 0.17 | 148.2 | 0.98 | 0.15 | 126.1 | 0.946 | 0.15 | 131.2 |
| 30 | 0.96 | 0.17 | 45.3 | 0.95 | 0.17 | 42.8 | 0.941 | 0.15 | 110.5 |
| 60 | 0.94 | 0.16 | 10.5 | 0.93 | 0.22 | 8.8 | 0.922 | 0.08 | 30.2 |
| 90 | 0.99 | 0.17 | 5.25997 | 0.91 | 0.23 | 4.21 | 0.932 | 0.1 | 10.8 |
| 110 | 0.92 | 0.15 | 3.07 | 0.82 | 0.12 | 2.96 | 1.01 | 0.07 | 7.5 |
| 130 | 0.94 | 0.17 | 2.67 | 0.97 | 0.12 | 2.5 | 0.99 | 0.01 | 5.2 |
| 150 | 0.90 | 0.16 | 2.28923 | 0.85 | 0.16 | 2.18 | 0.903 | 0.03 | 4.1 |

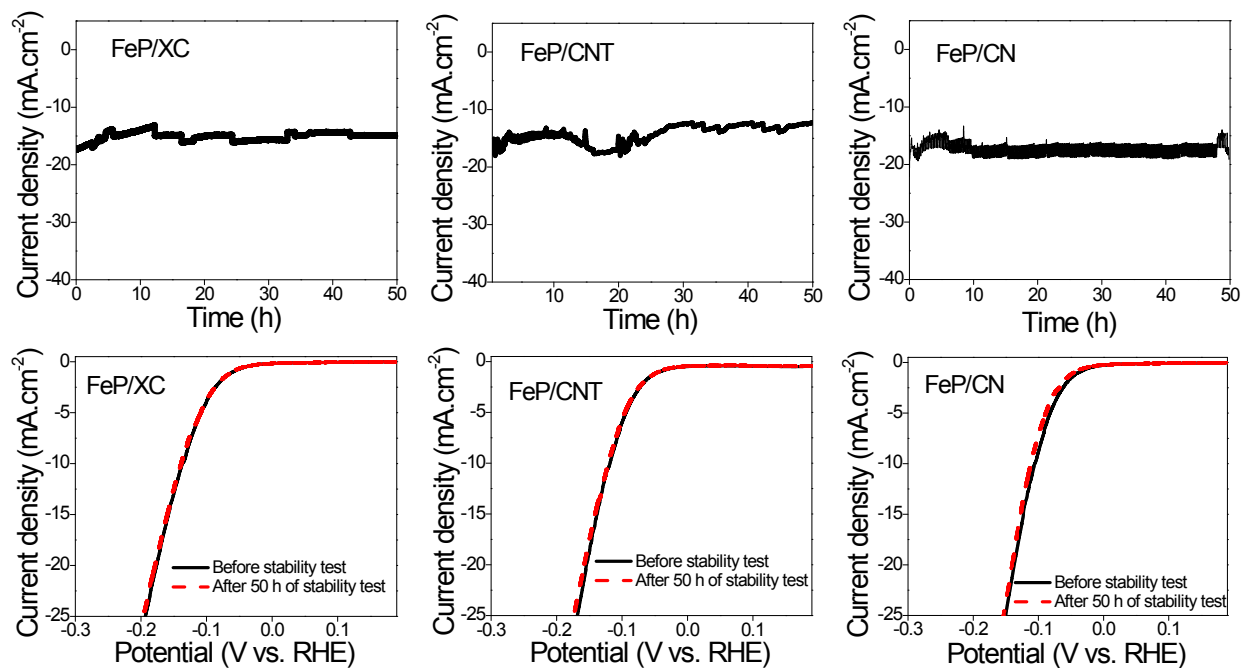


Fig. S15 Current-time and polarization curves obtained before and after potentiostatic experiments.